PRISM
Computational Sciences, Inc.

*Prism Computational Sciences, Inc.*
**455 Science Drive, Suite 140**
**Madison, WI 53711**

# Development of Ion Stopping Models for HED Plasmas Using Unified Self-Consistent Field Models and Self-Consistent Electron Distributions

**Final Report for the period: August 1, 2021 – July 31, 2022**

**Prepared for: Department of Energy, Office of Science, Fusion Energy Sciences (FES)**
**Award number: DE-SC0022112**

**I. E. Golovkin, Principal Investigator**

**Prism Computational Sciences, Inc.**

**PCS-R-180**

**October 2022**

## Contents

**Abstract**

We have implemented several corrections to the electronic stopping power model combining the RPA dielectric response formalism and local density approximation with electronic density distribution calculated in an average atom model. These modifications include strong collision correction, local field correction, electron binding energy correction, and the Barkas effect. The combined results bring the RPA-LDA stopping power in cold targets to closer agreements with experiments for a wide range of materials. The same method is then applied to the stopping of ions in warm dense plasmas.

The computational framework developed during this project is publicly available on GitHub (https://github.com/dedx-erpa/dedx). Tabulated data for protons in cold target for common materials are located in the data/ subdirectory of the repository.

## 1. Introduction

Ion stopping power is a fundamental transport property in plasma physics and plays a central role in a wide variety of high energy density laboratory plasmas (HEDLP) experiments, including charged particle energy deposition in fusion burn waves. Ion stopping power was extensively studied as a primary source of energy deposition in light ion beam fusion and remains of interest in heavy ion beam experiments to generate warm dense matter (WDM). The topic is especially relevant given the exponential growth in the use of ultrashort pulse laser (USPL) systems to accelerate beams of light and heavy ions to increasingly higher energies and intensities. Ion stopping power is central to the generation of many diagnostic signals as a result of inflight atomic and/or nuclear reactions. Accurate ion stopping power is essential in both kinetic simulations (e.g. Fokker-Planck collision operator) and as the "ion drag term" in multi-fluid plasma simulations. To advance our understanding of HEDLP science, it is vital to have high-fidelity stopping power and inflight reaction tools that are well-tested across relevant parameter spaces, and that are readily accessible to researchers in the HEDLP community. In the future it will also be important to have accurate stopping models for high-Z, non-protonic projectiles in plasmas of arbitrary composition, including high-Z plasmas. The main effort of the project has been the development and validation of a comprehensive, state-of-the-art ion stopping model for HED plasmas based on the finite temperature random phase approximation (RPA) formalism of Wang, Mehlhorn, and MacFarlane (Wang, Mehlhorn, and MacFarlane 1998) combined with the local density approximation as applied to electron distribution functions computed using the Flexible Atomic Code, FAC. This unified model avoids the unphysical jumps in stopping power that can occur when bound and free electrons are treated separately. The model was also extended to include temperature-dependent nuclear stopping in WDM. In the future, FAC could be used to generate data to implement models for the projectile effective charge in a plasma target, which has a quadratic impact on the stopping power. We have been developing and implementing strategies to perform rigorous model validation against a variety of data sets. For example, cold stopping data (e.g., NIST) has been used to evaluate the accuracy of the RPA model and explore inclusion of dynamical local field corrections and the Barkas effect. Our goal has been to provide a single comprehensive, efficient, and robust framework for computing energetic ion energy deposition and inflight reactions in HED plasmas spanning the relevant parameter space. We also hope to one day develop a module to implement in hydrodynamic and PIC codes. This would allow us to use HELIOS-CR to further test the validity of our plasma stopping power models against data from NRL, Sandia, and GSI stopping power experiments. This suite of codes will be useful to National Laboratories and universities (including several members of LaserNetUS network) for planning and analyzing HEDLP experiments. Our new models should significantly improve the fidelity of simulations involving ion stopping power and in-flight reactions.

We have delivered on our commitment to release e-RPA as an open-source standalone code for computing ion stopping powers and inflight reactions via GitHub, including the validation data sets. We have also begun communication with the developers of PlasmaPy about incorporating the code as an Affiliated Package. This will allow researchers to use the models and data within their own codes and applications, as well as to generate custom stopping power and reaction tables. In the future, these models could also be optimized for inclusion in hydrodynamic and PIC codes, such as HELIOS-CR. Such a combination of open source and commercial code and data will be particularly useful to the LaserNetUS, ICF, and pulsed power communities.

## 2. RPA dielectric response and local density approximation

In the dielectric response formalism, the electronic stopping power of an ion withe charge $z$ and velocity $v$ in a uniform electron gas of density $\rho$ can be written as,

$$S_e = -\frac{dE}{dx} = 4\pi \left(\frac{z}{v}\right)^2 \rho L(\rho, v) = \frac{2}{\pi}\left(\frac{z}{v}\right)^2 \int_0^\infty \frac{dk}{k} \int_0^{kv} d\omega\omega \mathrm{Im}\left(\frac{1}{\epsilon(k,\omega)}\right), \quad (1)$$

where $\epsilon(k, \omega)$ is the dielectronic response function, and $L(\rho, v)$ is the stopping function.

For electrons with non-uniform density distribution, we apply the local density approximation, and compute the total stopping power as:

$$-\frac{dE}{dx} = 4\pi \left(\frac{z}{v}\right)^2 \int d\vec{r}\rho(\vec{r})L(\rho, v). \quad (2)$$

In our model, the density distribution surrounding an ion is assumed to be spherical symmetric and calculated in the average atom model (AA) with a muffin-tin type potential, taking into account the screening effect of the continuum electrons. The Flexible Atomic Code (Gu 2008) has been used for the AA calculations. At finite temperature, the dielectric function in random phase approximation (Maynard and Deutsch 1985) is often used, and therefore we refer to the method as RPA-LDA approximation.

## 3. Various correction terms

Several correction terms are implemented to improve the accuracy and range of applicability of the RPA-LDA approximation.

First, the integration over the momentum transfer, $k$, must be truncated at certain maximum, $k_m$, above which the collisions become too strong for the perturbation theory underpinning the linear response formalism to be valid. The contribution for $k > k_m$ is instead calculated with the binary collision theory of Zwicknagel, Toepffer, and Reinhard (1999).

Second, the plasma coupling effect is included with a static local field correction function $G(k, \omega)$, by modifying the dielectric function,

$$\epsilon_{LFC}(k, \omega) = 1 - \frac{1-\epsilon(k,\omega)}{1+[1-\epsilon(k,\omega)]G(k,\omega)}. \quad (3)$$

We use the static local field correction function of Ichimaru and Tago (1981) for our models. Dynamic local field correction based on Mermin dielectric function, or some other

interpolation procedures were also tried, but it was not clear that those more complex methods are beneficial at all.

We also correct for the fact that RPA-LDA loss function $L(\rho, v)$ only depends on the local density and does not distinguish whether the electrons are bound or free. To that end, we introduce an effective electron density $\tilde{\rho}$, such that the loss function at any given radius is given by $L(\tilde{\rho}, v)$, and the effective density is defined through a correction to the plasma frequency,

$$\begin{aligned} \omega_p^2 &= 4\pi\rho \\ \widetilde{\omega_p}^2 &= 4\pi\tilde{\rho} \\ \widetilde{\omega_p}^2 &= \omega_p^2 + \gamma^2\omega_b^2, \end{aligned} \tag{4}$$

where $\omega_b$ is the mean binding energy of the electrons. In an average atom mode, and at any given radius, the electron density has contributions from different orbitals, although generally one or two subshell dominates. We calculate the mean binding energy as:

$$\ln\omega_b(r) = \sum_i f_i(r)\ln I_i \tag{5}$$

where $f_i(r)$ is the fractional contribution of the $i$-th bound shell at radius $r$, and $I_i$ is the binding energy of that shell. In this correction term, the empirical parameter $\gamma$ is adjusted to match experimental measurements of stopping powers in cold materials, and we found $\gamma^2 = 0.75$ provides the best fit.

Finally, the Barkas effect is estimated using the formalism developed in Esbensen and Sigmund (1990). However, the theory is based on perturbative expansion, and generally diverges at energies below the Bragg peak, we therefore use an empirical procedure to cutoff the correction term at low energies.

## 4. Comparison with experiments of cold targets

Our model contains several empirical parameters, such as $\gamma$ in the binding energy correction, and the cutoff energy of the Barkas effect. These parameters are adjusted by comparing the results with extensive experimental measurements of proton stopping power in cold targets. It is encouraging that a same set of parameters provide satisfactory fit to measurements over a wide range of atomic number. Figures 1 - 4 show the comparison of our calculated stopping powers of proton in C, Al, Ag, and Au with experimental results. It is seen that our model provides improved descriptions of the measurements over the original RPA-LDA method, especially at low energies and near the Bragg peak.

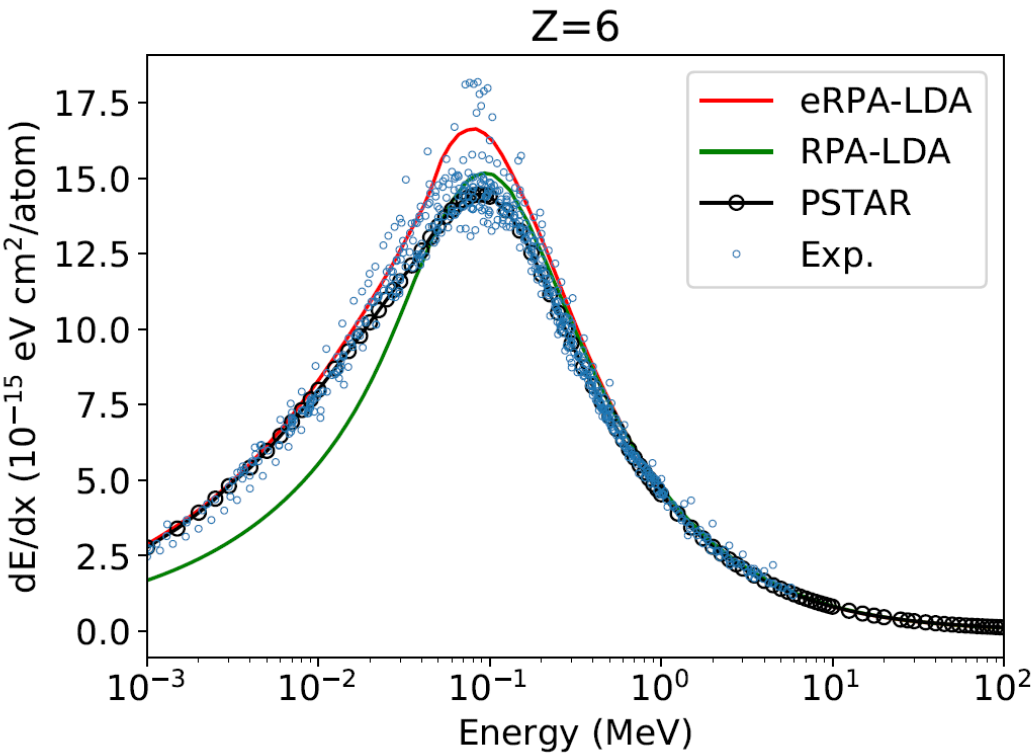


Figure 1. Comparison of calculated stopping power of proton in C target with experimental measurements.

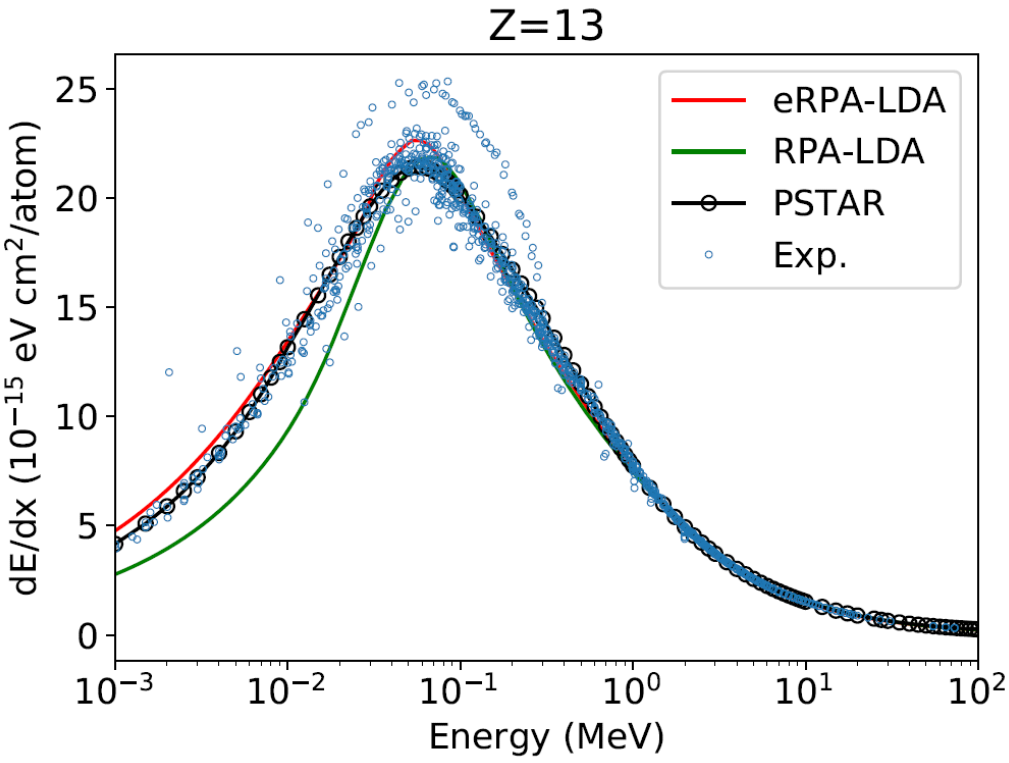


Figure 2. Same as Figure 1, but for Al.

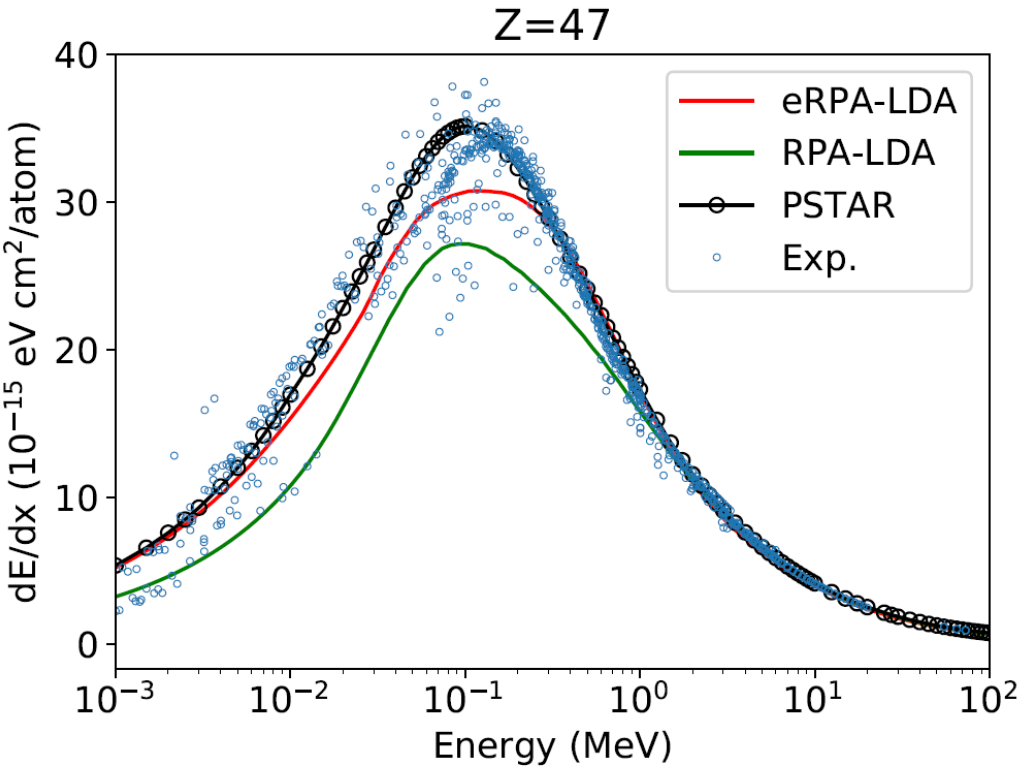


Figure 3. Same as Figure 1, but for Ag.

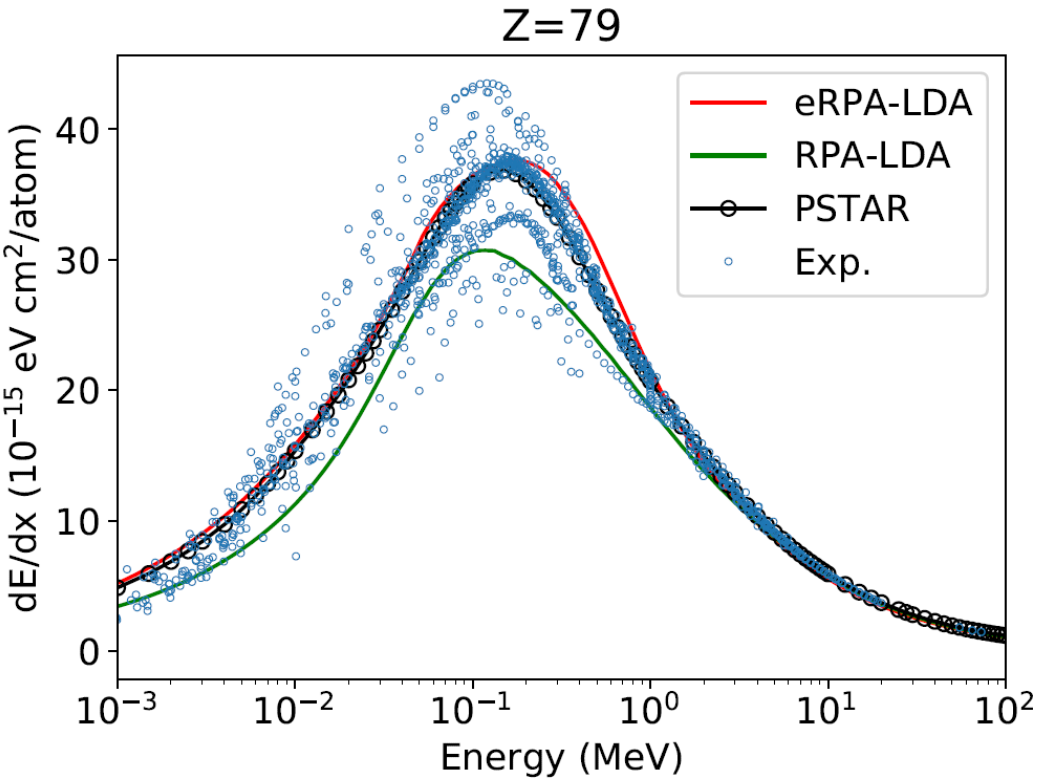


Figure 4. Same as Figure 1, but for Au.

It is interesting to show the relative contribution at different radii to the total stopping power at various projectile energies. Figure 5 shows the electron density profile, the loss function, the integrand in the LDA integral, and the fractional contribution to the stopping power within any given radius for the cold Al target, and proton energy of 1 MeV.

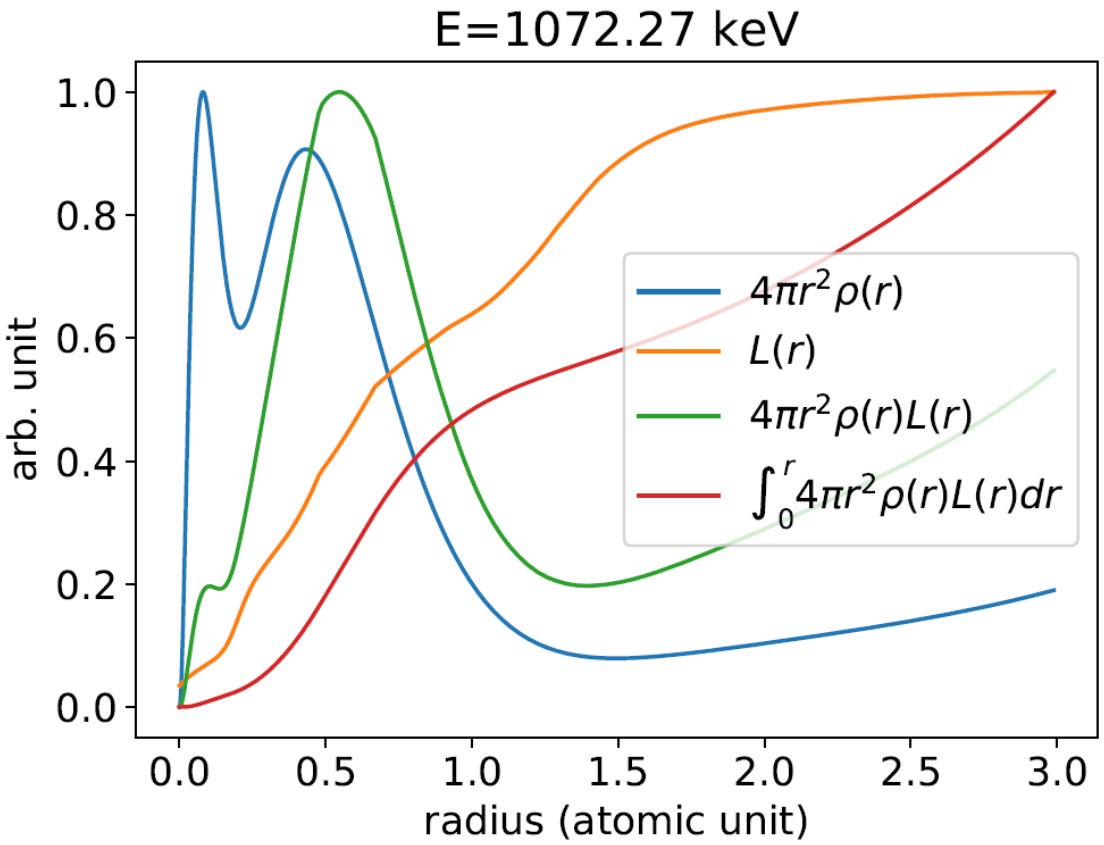


Figure 5. Contribution to total stopping power at different radius for cold Al target and proton energy of 1 MeV.

Figure 6 shows the same information for proton energy of 0.1 MeV. This shows the inner-shell electrons make smaller contribution to the stopping power at lower projectile energies.

Finally, Figure 7 shows the stopping ranges of proton in C, Al, Ag, and Au as functions of energy and comparison with PSTAR database.

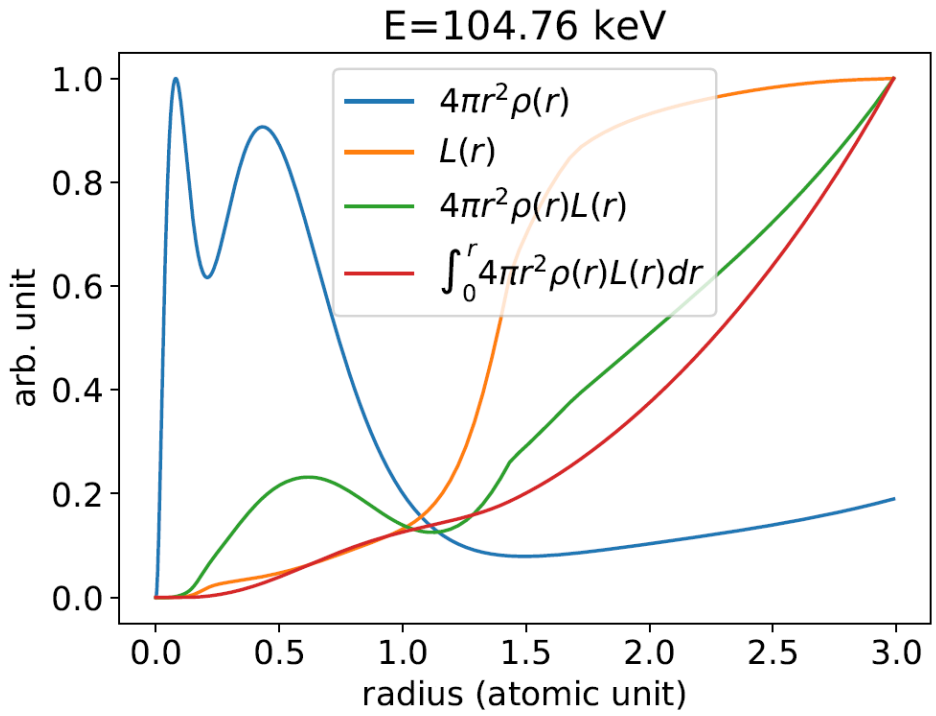


Figure 6. Same as Figure 5, but for proton energy of 0.1 MeV.

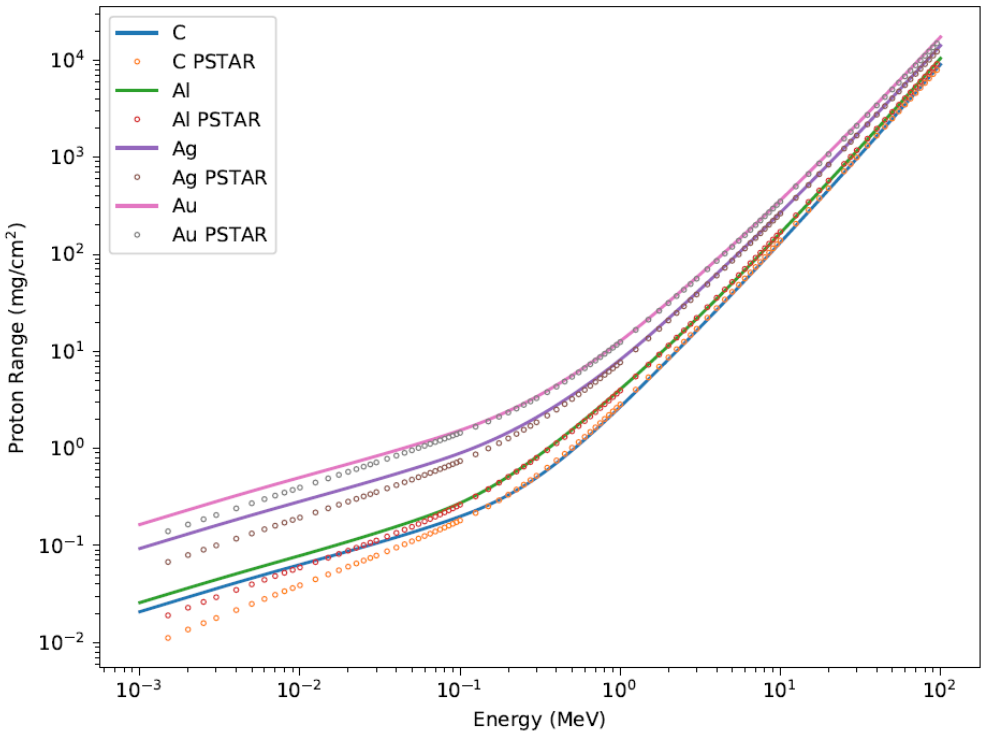


Figure 7. Proton stopping range in C, Al, Ag, and Au.

## 5. Stopping powers in warm dense plasmas

After calibrating our model using experimental results on cold targets, we apply it to warm dense plasma conditions. First, we compare the case discussed in the first charged-particle transport coefficient comparison workshop, where the stopping power of $\alpha$ particle in a uniform electron gas was presented. Figure 8 shows the comparison of our model with the quantum Gould-DeWitt (qGD) model for $n_e = 10^{25}$ cm$^{-3}$ and $T = 1$ keV.

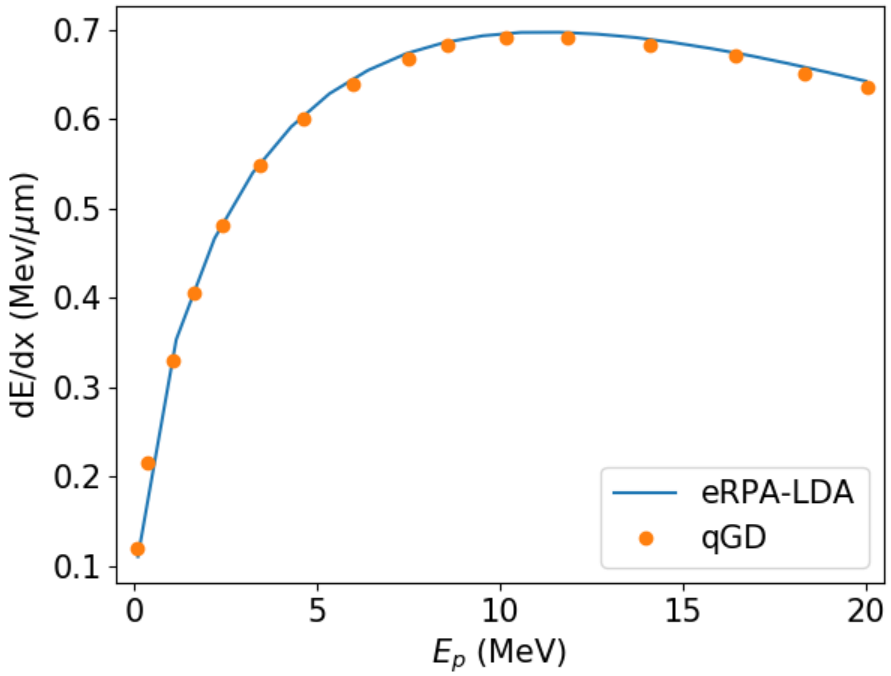


Figure 8. Stopping power of $\alpha$ particle in a uniform electron gas with $n_e = 10^{25}$ cm$^{-3}$ and $T = 1$ keV.

Figure 9 shows the temperature dependence of the stopping power for $n_e = 10^{25}$ cm$^{-3}$, and a projectile energy of 3.5 MeV.

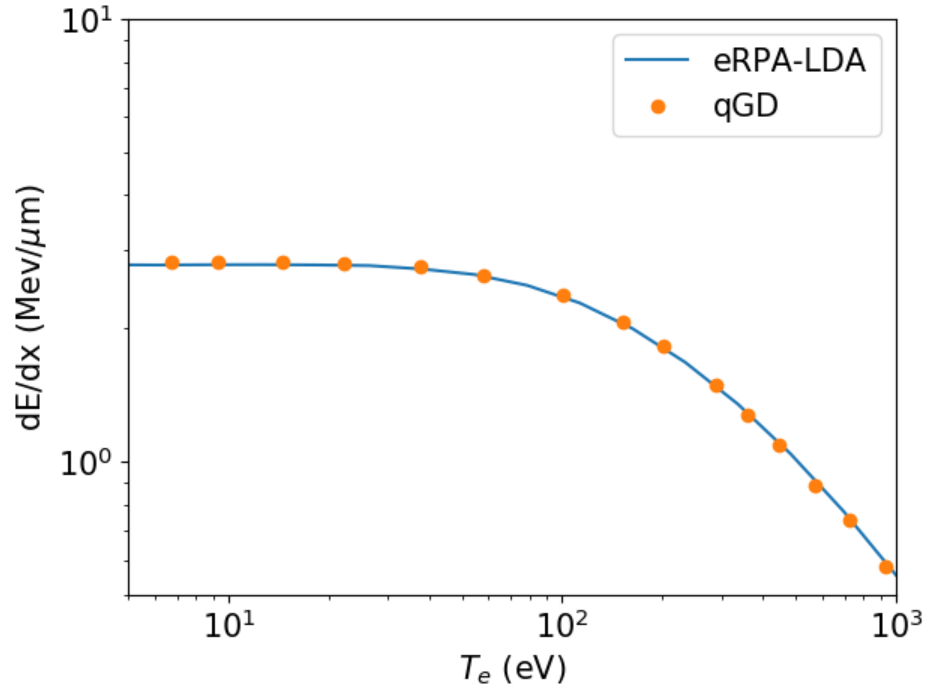


Figure 9. Same as Figure 8, but with a fixed projectile energy of 3.5 MeV and varying electron temperature.

Figure 10 shows the density dependence of the stopping power for $T = 1$ keV and projectile energy of 3.5 MeV.

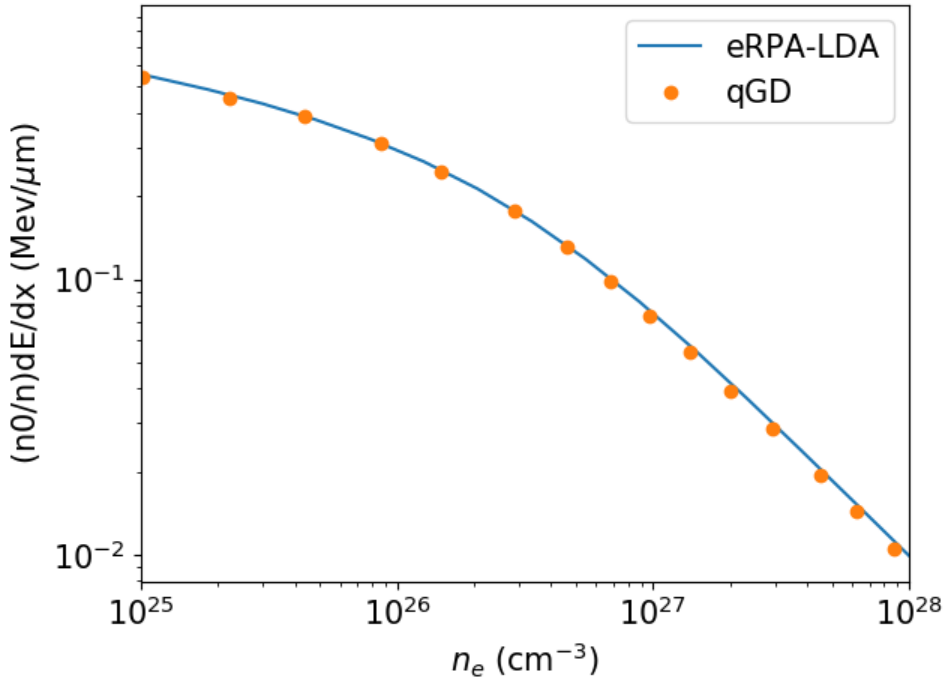


Figure 10. Same as Figure 8, but with a fixed projectile energy of 3.5 MeV and varying electron density.

Finally, there have been recent developments of applying density functional theory to the calculation of electronic stopping powers. White et al. (2021) used a mixed stochastic-deterministic time-dependent density functional theory (mDFT) to calculate the proton stopping power in a Carbon plasma at $T = 10$ eV and various densities. Figure 11 shows a comparison of our model and the mDFT results for Carbon density of 3.5 g/cc and $T = 10$ eV. The mDFT calculation only treats the $2s$ and $2p$ electrons in detail, and the $1s$ contributions are estimated with the model of Casas, Barriga-Carrasco, and Rubio (2013). However, it is seen that our model agrees well with the mDFT results without $1s$ contributions. We believe that the $1s$ contributions at energies near or below the Bragg peak should be completely negligible. It is therefore puzzling that White et al. (2021) shows the $1s$ contribution to increase at lower energies. To illustrate this fact further, figure 12 shows the radial dependence of the fraction contribution to the total stopping power of proton with energy of 33 keV (which corresponds to a velocity of 1.1 a.u.) in the Carbon plasma at $T = 10$ eV and density of 3.5 g/cc. The $1s$ electrons are mostly confined within $r < 0.5$, and our results indicate its contribution to the stopping power is less than 1% at this energy.

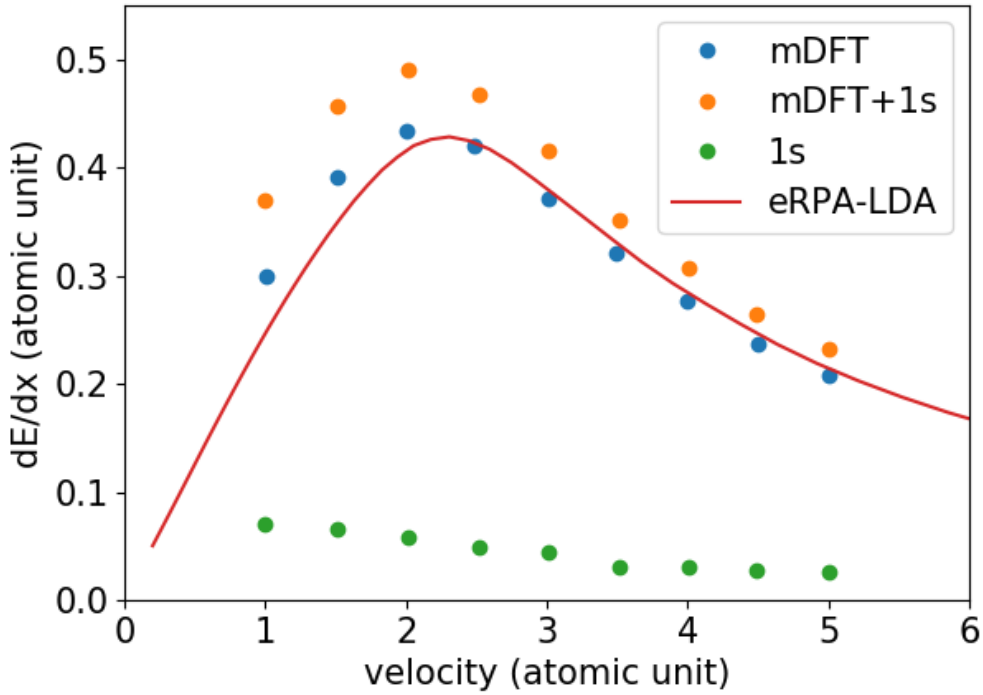


Figure 11. Stopping power of proton in a Carbon plasma with density 3.5 g/cc and temperature of 10 eV.

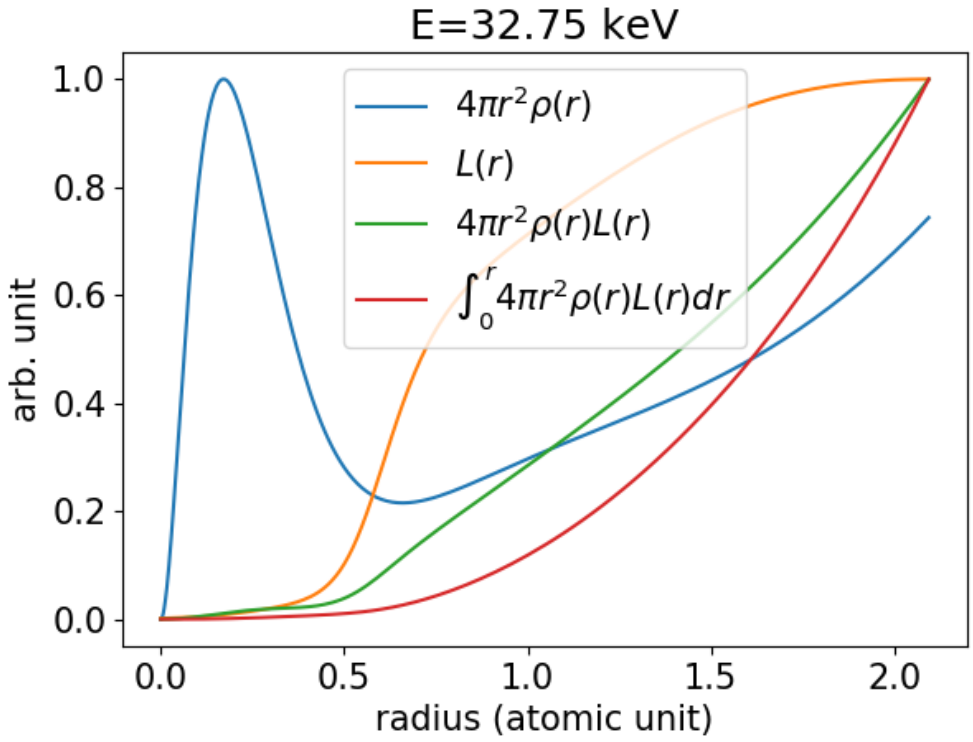


Figure 12. Fractional contribution to stopping power for proton in Carbon plasma.

Malko et al. (2022) presented recent experimental and theoretical results of proton stopping in a warm dense Carbon plasma with density of 0.5 g/cm$^3$, and temperatures of 10, 20, and 30 eV. For the covered proton energies, the density functional theory results show little temperature dependence, while several different theories show a wide variation of stopping powers near the Bragg peak. Figure 13 shows the comparison of DFT and the present model. This shows that our results are in close agreement with DFT calculations for these conditions.

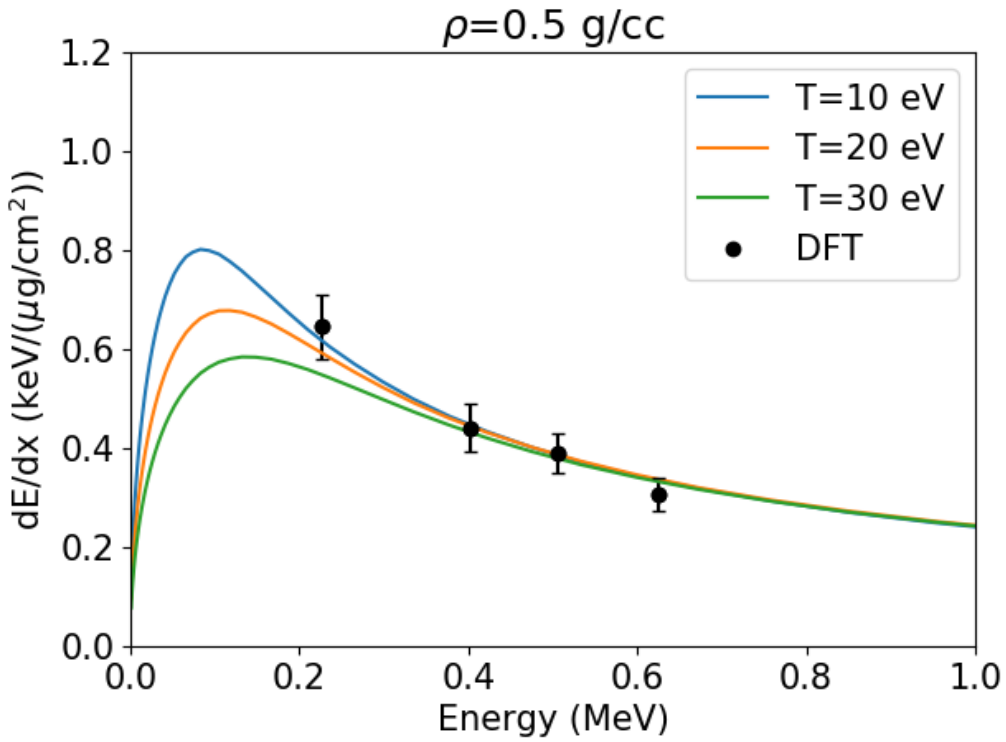


Figure 13. Stopping power of proton in a Carbon plasma with density 0.5 g/cc and temperatures of 10, 20, and 30 eV.

Young et al. (1982) measured energy loss of Deuteron in Mylar and Aluminum plasma at different temperature and densities. They reported no substantial enhancement in energy loss in Mylar for lower current density and 45% at the higher current density. For aluminum, the values were 20% and 40%. The present model predicts the energy loss at several plasma densities and temperatures corresponding to the experimental conditions.

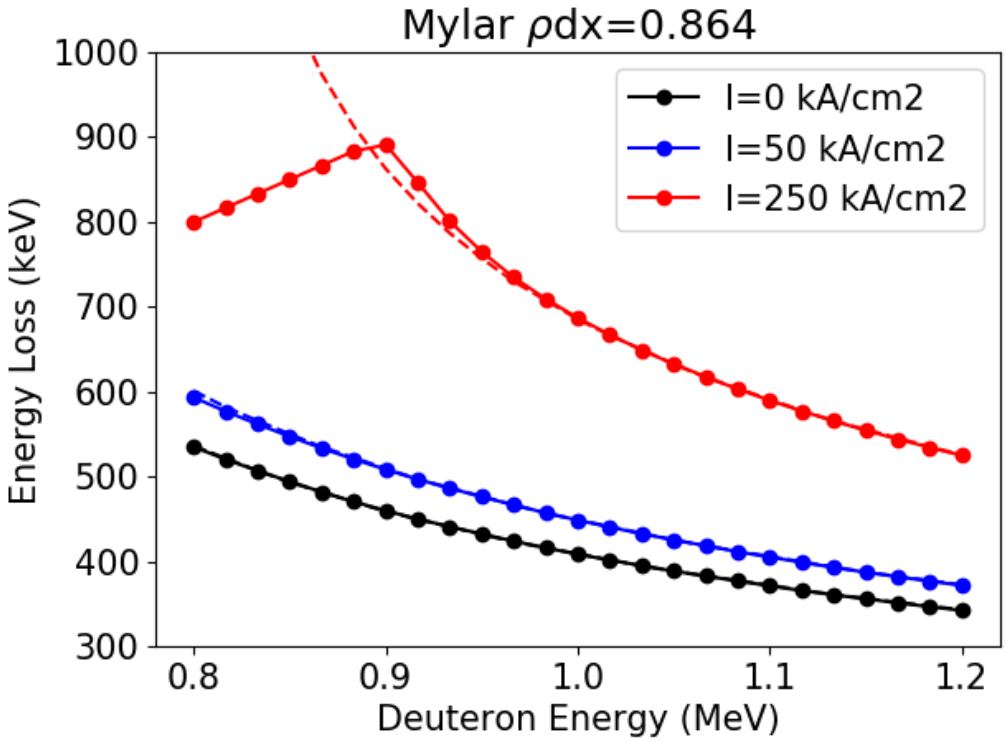


Figure 14. Energy loss of Deuteron in Mylar.

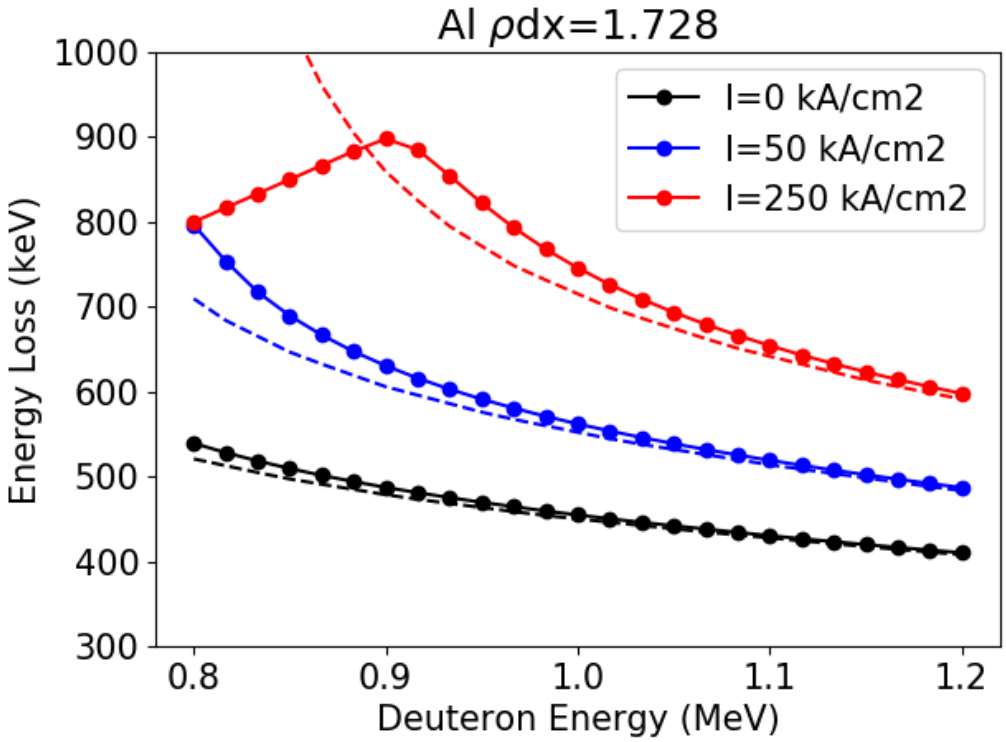


Figure 15. Energy loss of Deuteron in aluminum.

Olsen et al. (1985) analyzed the proton range in Nickel and Aluminum plasmas as a function of ionization charge. We calculated the range of 1.6 MeV proton in Ni and Aluminum at 1% solid densities over a wide range of temperatures. Figures 16 and 17 show the results as functions of the average ionization charge.

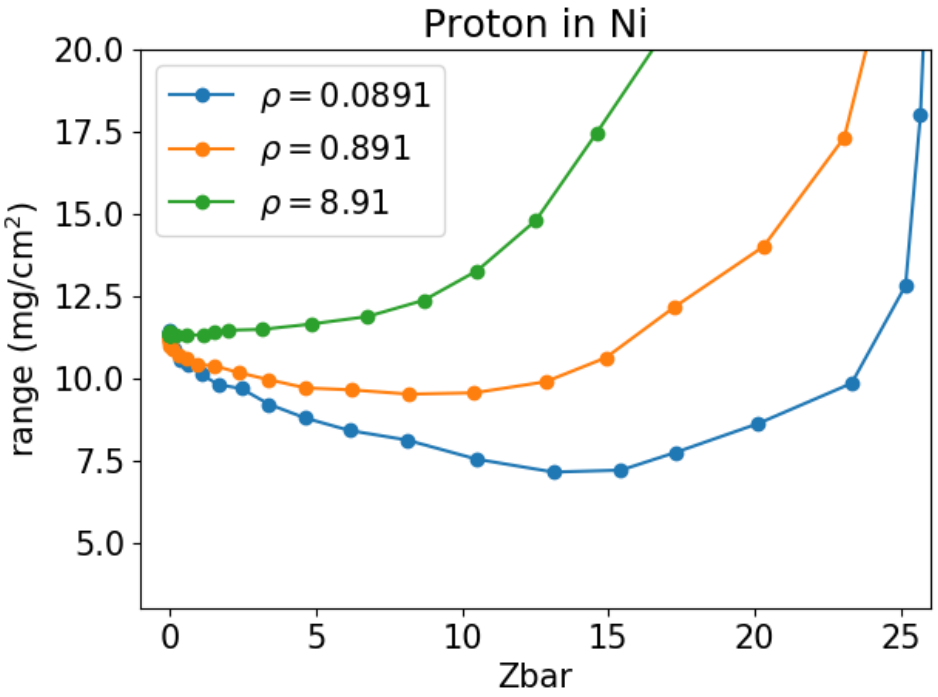


Figure 16. 1.6 MeV Proton range in Ni plasma as a function of average ionization charge.

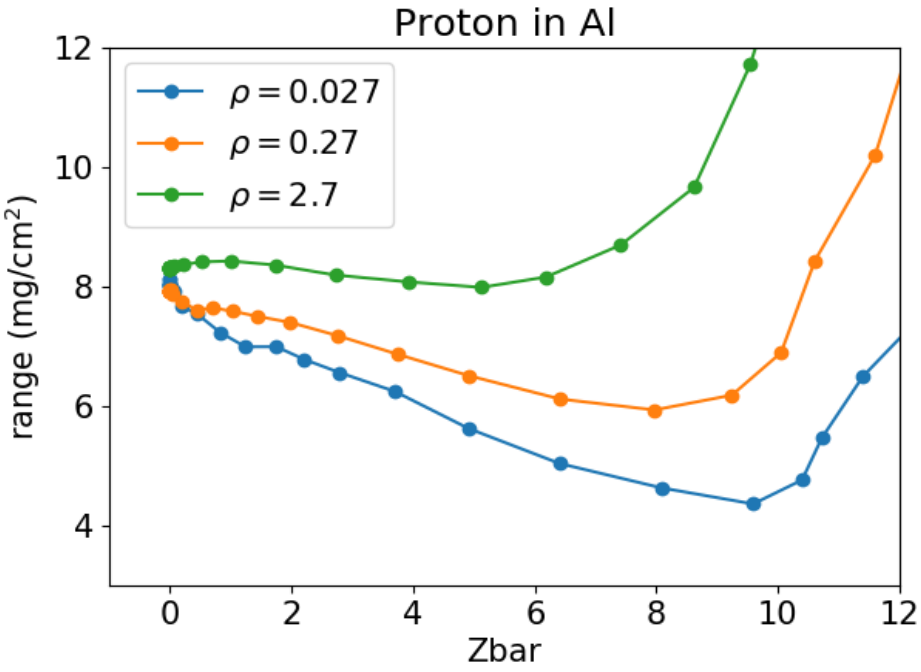


Figure 17. 1.6 MeV Proton range in Al plasma as a function of average ionization charge.

## 6. Summary and future work

We have reported on a new wide range electronic stopping power model that builds on the random phase approximation (RPA) dielectric response formalism of Wang, et al and the local density approximation (LDA) with electronic density distributions calculated in an average atom model using the Flexible Atomic Code (FAC). The accuracy of this model has been greatly improved by implementing several extensions to RPA theory including a strong collision correction based on the binary collision theory of Zwicknagel for $k>k_{max}$, a static local field correction, an electron binding energy correction, and the Barkas effect. The combined corrections bring our RPA-LDA proton stopping power results in cold targets into close agreement with experiments across the periodic table (PSTAR database). We have also shown results for the stopping of ions in warm dense plasmas as compared with the published data, including experiments performed in the 1980s as part of the NRL and Sandia Light Ion Beam Fusion Programs. Our work has focused on electronic stopping power, as this is most relevant for comparison with existing data and for alpha particle stopping in present day ICF targets on the NIF. We still plan to add the nuclear/ionic component of the stopping power to the model (Faussurier, Blancard, and Gauthier 2013) to enable alpha stopping calculations for alternative (exotic) nuclear fuel cycles where burn temperatures can exceed 30 keV and electron and ion contributions to the total stopping powers become equal.

We presented a talk on this work at the IEEE ICOPS meeting in Seattle (May 2022), as well as a poster at the APS DPP in Spokane (October 2022), where we also advertised our recent creation of a public GitHub site for gaining access to our open-source standalone code https://github.com/dedx-erpa/dedx). Tabulated data for protons in cold target are located in the data/ subdirectory of the repository. At APS DPP we also discussed how to add our e-RPA model into the PlasmaPy project. Nick Murphy and his colleagues plan to work with us to offer e-RPA as an Affiliated Package within PlasmaPy, which will help increase its visibility within the plasma physics community. We are also preparing an expanded version of the material in this report for submission as a peer-reviewed journal article, probably to Physics of Plasmas, where we will also advertise the availability of our open-source code.

We plan to continue to compare our model with a broader set of experimental data, including those highlighted in Figure 1 of Ref Malko et al. (2022). We have also been invited to submit a proposal for experiments on the ELIMAIA beam line (Prague) in conjunction with the HAPLS L3 1 PW laser, which would be used to generate plasma conditions We have formed a collaboration with Sophia Malko and Will Fox (PPPL), Suxing Hu (UR/LLE), and Luca Volpe (Centro de Laseres Pulsados (CLPU), Salamanca, Spain) and we will be submitting a contribution to the “Laser-Plasma Ion Sources at the ELIMAIA Beamline” or to the “Multidisciplinary Applications of Laser-driven Ions” workshops on November 2 and 4, 2022, respectively. This team will also explore submitting a proposal on ion stopping power to the LaserNetUS call (due December 19, 2022), as well as develop a plan for creating a dialog between TD-DFT calculations and our e-RPA model.

In our planning discussion about future experiments, we have had a request to incorporate our stopping power model into a version of Spect3D that can import the plasma conditions (density and temperatures) from hydrodynamic simulations of experiments to facilitate data analysis. This analysis tool, as well as further extensions of e-RPA will be considered for incorporation into proposals to DOE, NSF, and or AFOSR sponsors for support of stopping power experiments. We

also see utility to the user community in implementing this accurate ion stopping power model into an efficient and robust framework for computing ion energy deposition in HED plasmas spanning a wide range of temperatures and densities into both hydrodynamic and hybrid-PIC Monte Carlo codes. We were asked about this possibility by both WARP-X (LBNL/LLNL) and Triforce (UR/LLE) developers at the 2022 APS DPP. Prism's HELIOS-CR hydro code would be an excellent test bed for such a model. We also note that HELIOS-CR is used at universities and by the LaserNetUS community.

Finally, the US and international communities are revisiting the role of heavy ion accelerators in a future inertial fusion energy program. Accurate ion stopping power models are important for this community and we have had discussions with Thomas Schenkel (LBNL) about how our models and experimental data could be used to provide them validated models that they need to expeditiously focus on the critical path issues such as incorporating advanced accelerator technologies in power plant designs and using 3-D simulations to retire risk related to multiple beam focusing and combining. We note that supporting the heavy ion community will require the development of an open-source model for high-Z projectile charge states. Such a model is analogous to the collisional radiative equilibrium (CRE) models that are often supported by data generated by FAC, so we have the necessary expertise to generate such a model.

## 7. Acknowledgements

This work was supported by the U.S. Department of Energy, Office of Science, Fusion Energy Sciences (FES) under Award Number DE-SC0022112.

## 8. References


Casas, David, Manuel D. Barriga-Carrasco, and Juan Rubio. 2013. "Evaluation of slowing down of proton and deuteron beams in $CH_2$, LiH, and Al partially ionized plasmas" 88 (3): 033102. https://doi.org/10.1103/PhysRevE.88.033102.

Esbensen, Henning, and Peter Sigmund. 1990. "Barkas effect in a dense medium: Stopping power and wake field." *Annals of Physics* 201 (1): 152–92. https://doi.org/10.1016/0003-4916(90)90356-S.

Faussurier, Gérald, Christophe Blancard, and Maxence Gauthier. 2013. "Nuclear Stopping Power in Warm and Hot Dense Matter." *Physics of Plasmas* 20 (1): 012705. https://doi.org/10.1063/1.4774065.

Gu, M. F. 2008. "The flexible atomic code." *Canadian Journal of Physics* 86 (5): 675–89. https://doi.org/10.1139/P07-197.

Ichimaru, S., and K. Tago. 1981. "Wigner crystallization and the onset of a charge-density-wave instability in strongly coupled, classical, one-component plasma." *Journal of the Physical Society of Japan* 50 (February): 409–12. https://doi.org/10.1143/JPSJ.50.409.

Malko, S., W. Cayzac, V. Ospina-Bohórquez, K. Bhutwala, M. Bailly-Grandvaux, C. McGuffey, R. Fedosejevs, et al. 2022. "Proton stopping measurements at low velocity in warm dense carbon." *Nature Communications* 13 (May): 2893. https://doi.org/10.1038/s41467-022-30472-8.

Maynard, G., and C. Deutsch. 1985. "Born random phase approximation for ion stopping in an arbitrarily degenerate electron fluid." *J. Physique* 46: 1113–22.

Olsen, J. N., T. A. Mehlhorn, J. Maenchen, and D. J. Johnson. 1985. "Enhanced ion stopping powers in high-temperature targets." *Journal of Applied Physics* 58 (8): 2958–67. https://doi.org/10.1063/1.335844.

Wang, P., T. M. Mehlhorn, and J. J. MacFarlane. 1998. "A Unified Self-Consistent Model for Calculating Ion Stopping Power in Icf Plasma." *Physics of Plasmas* 5 (8): 2977–87. https://doi.org/10.1063/1.873022.

White, Alexander J., Lee A. Collins, Katarina Nichols, and S. X. Hu. 2021. "Mixed Stochastic-Deterministic Time-Dependent Density Functional Theory: Application to Stopping Power of Warm Dense Carbon." *arXiv E-Prints*, December, arXiv:2112.01638. http://arxiv.org/abs/2112.01638.

Young, F. C., D. Mosher, S. J. Stephanakis, Shyke A. Goldstein, and T. A. Mehlhorn. 1982. "Measurements of Enhanced Stopping of 1-MeV Deuterons in Target-Ablation Plasmas" 49 (8): 549–53. https://doi.org/10.1103/PhysRevLett.49.549.

Zwicknagel, Günter, Christian Toepffer, and Paul-Gerhard Reinhard. 1999. "Stopping of heavy ions in plasmas at strong coupling" 309 (3): 117–208. https://doi.org/10.1016/S0370-1573(98)00056-8.